Glucan Particles Loaded with Fluorinated Emulsions: A Sensitivity Improvement for the Visualization of Phagocytic Cells by 19F-MRI

(Article begins on next page)

27 September 2023

Glucan Particles Loaded with Fluorinated Emulsions: a Sensitivity Improvement for the Visualization of Phagocytic Cells by ^{19}F-MRI

Cristina Chirizzi[a], Walter Dastrù[a,b], Daniela Delli Castelli[a], Valeria Menchise[b], Silvio Aime[a,b], Enzo Terreno[a,b,*]

[a]Molecular & Preclinical Imaging Centers, Department of Molecular Biotechnology and Health Sciences, University of Torino, Torino, Italy;
[b]Istituto di Biostrutture e Bioimmagini CNR, UOS c/o Molecular Biotechnology Center, Torino, Italy

Abstract: A protocol to load perfluoro-crown-ether (PFCE) nanoemulsion directly into yeast-derived glucan particles (GPs) was developed. It was observed that the PFCE encapsulation did not affect the ^{19}F-MRI properties of the nanoemulsion that is currently in clinical trials. GPs loaded with PFCE nanoemulsion were taken up avidly by murine macrophages *in vitro*, resulting in a cellular uptake 150 % higher than the not GPs-entrapped nanoemulsion. Accordingly, a corresponding improvement in the ^{19}F-MRI detection of the labelled cells can be obtained. The high biotolerability and versatility of GPs, makes these microcarriers a promising option for designing of improved *in vivo* cellular imaging protocols.

1. INTRODUCTION

The last two decades have witnessed a growing interest in cell-labeling procedures for pursuing the *in vivo* visualization with imaging scanners. Among the the different available imaging modalities, Magnetic Resonance Imaging (MRI) is the most suitable for cell tracking experiments.[1-3] This low-invasive technique provides very high resolution images and the possibility to visualize the whole body without any problems of tissue penetration. Cells can be labelled both *in vitro* and *in vivo*. In the former approach, the imaging probe is introduced into cells in a controlled cell culture environment prior to cells injection/transplantation. Differently, *in vivo* labelling consists of the systemic injection of the probe, typically nanoparticles, which is recognized and internalized by specific cell populations (*e.g.* blood circulating monocytes/macrophages).

The relatively poor sensitivity of MRI requires the internalization of high amounts of these probes in the cells, regardless of the selected labelling method.

The most used class of MRI probes for cellular imaging is represented by iron oxide nanoparticles (IONPs).[4,5] Such particles, being negative contrast agents, generate a T_2/T_2^* weighted signal loss. Therefore, the detection of labelled cells can be quite challenging in organs with an intrinsically low MRI signal (*e.g.* lung, bones) or in the presence of haemorrhages (because of the paramagnetism of de-oxy haemoglobin). Furthermore, the IONP-labelled cells generated contrast is linearly correlated to the cells number only at low iron concentrations.[6,7]

The drawbacks associated with the signal loss can be overcome by using positive contrast T_1 agents, and several preclinical studies have demonstrated the potential of Gd-complexes in cellular imaging.[8,10] However, the detection sensitivity of Gd-labelled cells is lower than IONPs, and also the quantitative analysis is very challenging. Another approach consists of labelling cells with CEST (Chemical Exchange Saturation Transfer) contrast agents,[10,11] even if more work is still necessary to assess the real clinical potential of this class of contrast media.

A new emerging approach for cellular MRI is based on the use of fluorine-containing agents (^{19}F, 100% natural abundance).[12,13]

[19]F-based MRI has gained great attention in the last 20 years, especially for the possibility to obtain quantitative information (absence of background signal), which allows specific and selective detection of

the administered ^{19}F-containing probes.[14,15] Moreover, the chemical shift of ^{19}F is spread out over a wide range, thus allowing the design of multiplex imaging protocols where different agents present in the same anatomical region can be individually visualized.[16] Because of their high payload of ^{19}F atoms and good biotolerability, perfluorocarbons (PFCs) nanoemulsions are the most frequently used ^{19}F-MRI contrast agents in biomedical imaging. Several studies have demonstrated the potential of PFCs to label and image cells (mostly phagocytic) either *in vitro* or *in vivo*.[17,18] Very important, the clinical relevance of cellular ^{19}F-MRI, especially for quantification purposes, has been recently demonstrated on humans.[19]

The aim of this work was to improve the detection sensitivity in ^{19}F-MRI cellular imaging experiments through the entrapment into Glucan Particles (GPs) of a nanoemulsion made of perfluoro-crown-ether (PFCE), which is the agent currently in clinical trials. GPs are hollow porous shells derived from *Saccharomyces cerevisiae.* Up to now, they have been mainly investigated as innovative platform for oral vaccines,[20] and for macrophage-directed drug delivery.[21-23] More recently, they have been demonstrated to be highly biocompatible microcarriers with a good potential for *in vivo* cellular imaging, especially for the visualization of immune cells.[24-26]

2. MATERIALS AND METHOD

2.1 Chemicals

Rhodamine-DSPE was purchased from Avanti Polar Lipids (Alabaster, AL, USA).

All the other chemicals were purchased from Sigma Aldrich (St. Louis, MO, USA) and used without any purification.

Cell culture medium components (Dulbecco Modified Eagle Medium – DMEM – and Fetal Bovine Serum - FBS) were purchased from Lonza.

2.2 Preparation of PFCE-NE and Rho-PFCE-NE

The PFCE-based nanoemulsion was produced by emulsifying perfluoro-15-crown-5-ether (PFCE) with Pluronic F-68 by a direct sonication with a Bandelin Electronic UW2070 sonicator tip. A 200 mM PFCE mixture in Pluronic F-68 (2% v/v in water) was prepared and sonicated by employing two cycles of 30 seconds at 50% of power followed by two cycles of 30 seconds at 70% of power.[27] The fluorescent nanoemulsion (Rho-GP-PFCE-NE) was prepared adding 0.1 mol% of the lipophilic fluorescent dye Rhodamine-DSPE to PFCE before the emulsification with Pluronic F68.
The hydrodynamic diameter of the nanoemulsion and the polydispersion index (PDI) was determined by dynamic light scattering (DLS) (Zetasizer Nano ZS, Malvern, UK).

2.3. Preparation of GPs

Glucan particles were prepared according to the procedure first described by Soto and Ostroff.[28] 100 g of *Saccharomyces cerevisiae* were suspended in 1 L of 1 M NaOH and heated to 80°C for 1 h. The insoluble material consisting of the yeast shells was collected by centrifugation at 2000 g/min for 10 min. It was then suspended in 1 L of water, brought to pH 4–5 with HCl, and incubated at 55°C for 1 h. The insoluble residue was again collected by centrifugation and washed once with 1 L of water, four times with 200 mL of isopropanol, and twice with 200 mL of acetone. The resulting slurry was placed in a glass tray and dried at room temperature to produce 12.4 g of a fine, slightly off-white powder.

2.4. Entrapment of PFCE-NE in GPs

50 mg of dry GPs were suspended in 200 µL of PFCE (or PFCE + Rhodamine-DSPE) and left under stirring at RT overnight to allow the entrance of PFCE into the particles core. Next, 2.9 mL of a Pluronic F-68

solution (2% v/v in water) were added to the GPs suspension resulting in a biphasic system that was emulsified by sonication (2 cycles of 30 sec, power 50%, followed by 2 additional cycles of 30 sec, power 70%). A final fluorine concentration of 4 M was obtained. Untrapped PFCE-NE was removed by washing (10x) with isotonic HEPES buffer (pH = 7.4). Finally, the GP-loaded nanoemulsion was suspended in 1 mL of isotonic HEPES buffer.

The loading efficiency (PFCE-NE entrapped/PFCE-NE incubated) was evaluated by ^{19}F-NMR spectrometry. A tube containing the GP-PFCE-NE suspension was added with a known amount of trifluoroacetic acid (TFA) used as internal reference. After acquiring the NMR spectrum (Bruker Avance 300), the amount of fluorine entrapped in GPs was determined by integration with respect to the TFA signal.

2.5 Cellular uptake experiments

Macrophages J774.A1 were generated from *Mus musculus* ascites from reticulum cell sarcoma. The base medium for this cell line is DMEM supplemented with 10% FBS, 100 U/mL penicillin, 100 µg/mL streptomycin and 5 mM of glutamine. Cells were grown at 37 °C in a humidified atmosphere containing 5% CO2.

About 2 million of J774.A1 cells were seeded in 6 cm culture dishes. One day after seeding, cells were washed and incubated for two hours at 37 °C with PFCE-NE or with GP-PFCE-NE (or Rho-GP-PFCE-NE) solutions, both at a fluorine concentration of 100 mM in DMEM. After incubation, cells were washed ten times with PBS, detached with a manual scraper and transferred in glass capillaries, which were centrifuged to obtain a cell pellet suitable for ^{19}F-MRI experiments. The number of cells was evaluated by determining the protein concentration of the cell lysates by commercial dye-binding Bradford assay (Biorad, Hercules, CA, USA).

2.6 ^{19}F-MRI measurements

^{19}F-MRI experiments were performed on a Bruker Avance300 working at 7 T and equipped with microimaging probes. The pulse sequence providing the highest S/N ratio for the herein reported systems was a fast spin echo (RARE) with the following parameters: TR=1500.00 ms, TE= 5.64 ms, RARE factor = 32, Field of view = 25 mm, slice thickness = 1.5 mm, matrix size 32x32. As far as quantification of the fluorine content was concerned, a capillary containing a known amount of PFCE was inserted into the phantom as reference. The signal to noise ratio (SNR) has been determined as follows:

$$SNR = \frac{I - I_B}{STD_B}$$

where I is the intensity of the ^{19}F signal in the region of interest, I_B is the intensity of the background signal and STD_B is the standard deviation of the background signal.

2.7 Fluorescence confocal microscopy

After 24 hours from seeding, cells were incubated at different times (1, 2 and 3 hours) with Rho-GP-PFCE-NE 100 mM in fluorine. Confocal microscopy analysis was performed using Laser Scanning Confocal Microscopy (Leica TCS SP5, Leica Microsystem Srl.). Experiments were carried out using a 20x dry lens and a 63x oil-wet lens. The rhodamine-based dye was visualized in the red channel ($\lambda_{ex}/\lambda_{em}$ 561nm/583 nm).

4. RESULTS AND DISCUSSION

The aim of this work is the design and testing of GPs loaded with a fluorinated nanoemulsion made of per-fluoro-15-crown-5-ether (GP-PFCE-NE) to increase the cell uptake efficiency and, consequently, the detection sensitivity for the ^{19}F-MRI visualization of phagocytic cells.

The experimental procedure to entrap the nanoemulsion in GPs is described in detail in Subsection 2.4. Glucan particles are very stable and insoluble in any solvent and their shell is highly porous, thus allowing the free passage of small-sized molecules.[29] The method for entrapping PFCE nanoemulsion (PFCE-NE) in GPs started with suspending the glucan particles in neat PFCE to pursue a non specific distribution of the fluorinated compound between the particle cavity and the bulk. Then, PFCE-NE was formed (both inside and outside the particles) following a sudden change of polarity of the suspending medium caused by the addition of an aqueous solution of the surfactant Pluronic F68. Finally, centrifugation and exhaustive washing allowed for the separation of the GP-entrapped and the non-entrapped nanoemulsion.

The hydrodynamic diameter of PFCE-NE (determined by DLS) was 199.4 nm with a polydispersion index of 0.11, in good agreement with those reported in literature for similar formulations.[27]

The ^{19}F-NMR spectrum of GP-PFCE-NE was characterized by a single resonance at -16.5 ppm (using TFA as reference, Figure 1), exactly as observed for the not entrapped PFCE-NE. The isochronicity of all the twenty fluorine atoms per molecule in the emulsion is certainly an important advantage for the intended imaging applications, because it improves sensitivity detection.
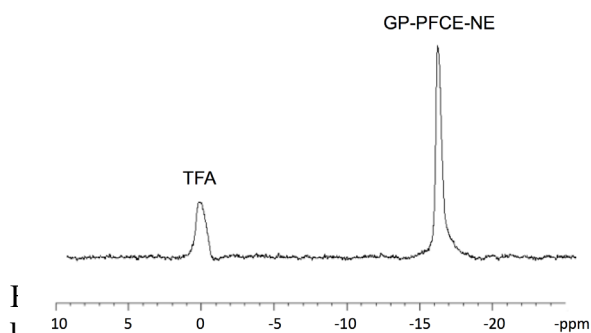
I .... iture) of GP-PFCE-NE. (trifluoroacetic acid, TFA, was

The loading efficiency of the fluorinated compound (GP-entrapped *vs.* incubated PFCE) was evaluated by integrating ^{19}F-NMR spectra using a stock solution of TFA as internal reference. A total fluorine amount of 0.52 millimoles was estimated for the GP-PFCE-NE suspension. As the amount of fluorine in the solution used for the incubation with empty GPs was 12.3 millimoles, a loading efficiency of 4.2% was obtained. This number is lower than the corresponding value obtained for amphiphilic Gd-complexes (even considering the different amount of GPs used in the preparation).[29] Most likely, the co-entrapment of the surfactant (not necessary for the Gd-complex) accounts for this difference. Conversely, the loading efficiency reported for fluorescent dyes is much higher (60-70%), but in that case very small amounts of material (< 100 nanomoles) were dissolved in the suspension of GPs.[26]

On the other hand, the loading content (*i.e.* mass of GP-entrapped PFCE *vs.* mass GPs) of the final suspension was 30%, which is much higher than the GPs formulations with Gd-complexes (1-2%) or fluorescent dyes (< 0.1 %). The loading content is directly correlated to the absolute concentration of the material to be entrapped, thus justifying the large number obtained.

Due to the relatively large dimensions of GPs, the number of particles in the suspension was counted by optical microscopy and resulted to be 4.2×10^9 ml^{-1}. Thus, the estimated number of fluorine atoms per particle corresponded to 5.7×10^{11}. It is worth mentioning that this number is *ca.* two-order of magnitude higher than the number of paramagnetic Gd ions that were entrapped in GPs.[29]

The comparison between longitudinal (T$_1$) and transverse (T$_2$) ^{19}F relaxation times (7 T, 25°C) of PFCE-NE and GP-PFCE-NE suspensions (Table 1) indicated that, in analogy to the chemical shift values, also the

relaxation times of the nanoemulsion was unaffected by the entrapment in GPs. Furthermore, the values are in good agreement with the data reported in literature for PFCE-based nanoemulsions.[16]

Table 1. Longitudinal (T_1) and transverse (T_2) relaxation times of ^{19}F-PFCE-NE (25°C, 7 T).

Sample	T_1 (s)	T_2 (s)
PFCE-NE	0.80	0.29
GP-PFCE-NE	0.83	0.32

In order to compare the ^{19}F-MRI detection sensitivity between PFCE-NE and GP-PFCE-NE, phantoms of the two samples containing different fluorine concentrations (from 10 to 40 mM) were prepared, suspended in agarose gel, and imaged at 7 T and room temperature.

Figure 2 (top) reports the ^{19}F-MR image of the GP-PFCE-NE phantoms. The ^{19}F-MR signal, expressed as SNR (Figure 2, bottom) indicates that the detection sensitivity in this experimental setting (see section 2.5) was somewhere between 10 mM and 20 mM of fluorine. The same result was obtained for the PFCE-NE phantom (data not shown).

The obtained result confirmed the good quantification capability of the technique.

Next, the relative cell labelling efficiency of the two ^{19}F-agents was measured *in vitro*. To this purpose, an immortalized cell line of murine macrophages (J774.A1) was chosen. About 2 millions of cells, suspended in 3 ml of culture medium, were incubated for 2 hours at 37 °C in presence of PFCE-NE or GP-PFCE at a fixed concentration of fluorine (100 mM). Then, labelled cells were washed and pelleted in glass capillaries (2 mm of diameter) and subjected to ^{19}F-MRI. To quantify the amount of cell-internalized fluorine in each sample, a capillary containing PFCE-NE at 1 mM was used as external standard.
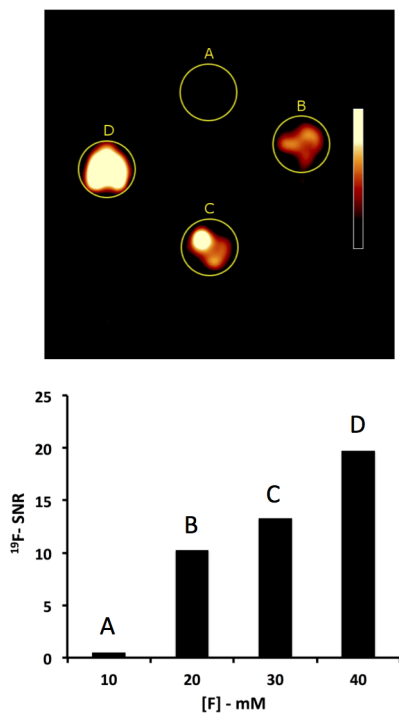

Figure 2: Top: ^{19}F-MR image of a phantom containing different amount of GP-PFCE-NE. Bottom: corresponding signal-to-noise ratio values.

The obtained images (Figure 3) clearly indicated that the ^{19}F-MRI signal of GP-PFCE-NE was higher than the one observed for PFCE-NE, thus suggesting an increase of the amount of fluorine internalized in the cells when the nanoemulsion is entrapped in GPs.

An estimation of the number of fluorine atoms per cell was calculated from the intensity of the signal of the reference sample.

The amount of fluorine internalized in J774.A1 cells *via* GPs was more than doubled with respect to the number obtained using the free nanoemulsion as labelling agent (1×10^{12} *vs.* 4×10^{11} F atoms/cell, respectively). Considering that the number of fluorine atoms entrapped in a single glucan particle is 5.7×10^{10}, it can be concluded that an average of 20 GPs were internalized in the macrophages.

Although the amount of fluorine internalized in a single cell can be largely affected by a vast array of factors (*e.g.* agent type and concentration in the incubation medium, incubation time, cell type), the number obtained in this work falls among the upper values in the range (10^{11}-10^{12} F atoms/cell) generally pursued in the labelling of different cell types (stem cells, phagocytic or non-phagocytic cells, with human or murine origin) using perfluorinated nanoemulsions.[12,19,30]

The excellent uptake observed using fluorinated GPs is most likely the result of the active targeting displayed by □-1,3-D glucan moieties towards specific receptors like dectin-1 (D1) and complement-receptor 3 (CR3) that are expressed by macrophages.[31,32] Such receptors are not recognized by PFCE-NE.
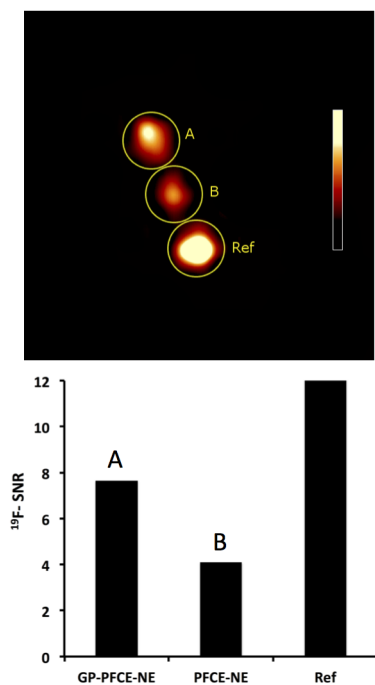

Figure 3. Top: ^{19}F-MR image of a phantom containing J774.A1 cells labelled with GP-PFCE-NE (A), PFCE-NE (B). A capillary containing 1 mM of PFCE-NE was used as internal reference (Ref). Bottom: corresponding signal-to-noise ratio values.

To assess the detection threshold for the cells labelled with GP-PFCE-NE, a phantom consisting of five capillaries filled with the same total number of J774.A1 cells, but containing a different fraction of labelled macrophages, was subjected to a ^{19}F-MRI session.

The results reported in Figure 4 indicated that, in the used imaging setup, the presence of 5% of labelled cells in a pellet is still detectable. That sample contained 2500 labelled cells/□L.

To visualize the intracellular localization of the fluorine-rich GPs, a formulation of PFCE-NE loaded with 0.1 % (in moles) of the lipophilic fluorescent dye Rhodamine-DSPE (Rho-PFCE-NE) was prepared (see subsections 2.2 and 2.4).

The fluorescent particles were incubated for different times (1 h, 2 h, and 3 h) with J774.A1 macrophages following the same procedures described in subsection 2.5. Then, the labelled cells were observed by fluorescence confocal microscopy. The images reported in Figure 5 indicated that already after 1 h of incubation, most of the cells internalized the particles. Although the cellular uptake significantly increased over time, the fluorescent signal did not show diffusion, thus suggesting that the particles did not release their payload after 3 hours. Interestingly, the number of internalized particles can be counted, and the result agrees well with the number calculated from ^{19}F-MRI analysis.
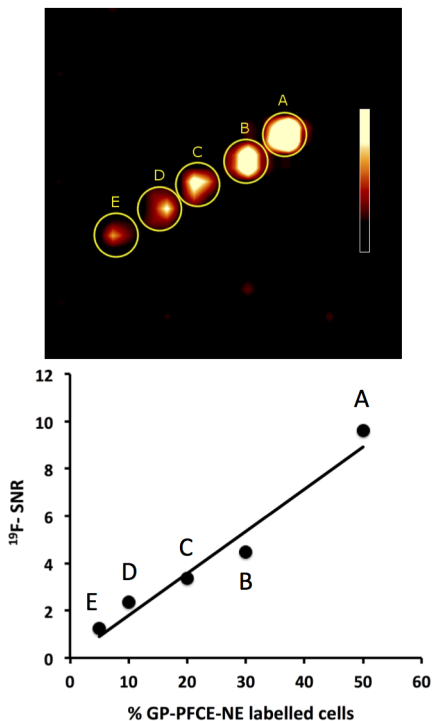

Figure 4. Top: ^{19}F-MR image of a phantom of capillaries containing different amounts of J774.A1 cells labelled with GP-PFCE. Bottom: corresponding signal-to-noise ratio values. The line indicates the good linearity between 19F-MRI signal and number of labelled cells.
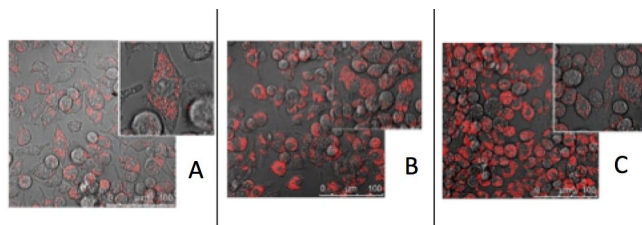

Figure 5. Confocal fluorescence microscopy images of J774.A1 cells labeled with GP-Rho-PFCE-NE. Cells were observed after 1h (A), 2h (B) and 3h (C) of incubation time.

5. CONCLUSION

In summary, in this work we presented a novel ^{19}F-MRI contrast agent specifically suitable for labeling and tracking phagocytic cells. The probe is represented by microsized yeast-derived glucan shells loaded with nanoemulsion made of a fluorinated molecule already tested on humans. The fluorine uptake and, consequently, the ^{19}F-MRI detection sensitivity of macrophages labeled with the fluorinated glucan particles, was more than two-fold higher than the PFCE agent currently in clinical development. Furthermore, it has been reported that glucan particles are very well tolerated by cells,[24] and can be successfully used for both *in vitro* or *in vivo* cellular imaging experiments.[26]

LIST OF ABBREVIATIONS

PFCE: Perfluoro-15 Crown-5 Ether

GPs: Glucan Particles

MRI: Magnetic Resonance Imaging

IONPs: Iron Oxide NanoParticles

CEST: Chemical Exchange Saturation Transfer

PFCs: PerFluoroCarbons

DSPE: Di-Stearoyl-Phosphatidyl-Ethanolamine

DMEM: Dulbecco Modified Eagle Medium

FBS: Fetal Bovine Serum

Rho: Rhodamine

DLS: Dynamic Light Scattering

PDI: PolyDispersity Index

PFCE-NE: Perfluoro-15 Crown-5 Ether NanoEmulsion

GP-PFCE-NE: Glucan Particle loaded Perfluoro-15 Crown-5 Ether NanoEmulsion

TFA: TriFluoro Acetic acid

NIRF: Near InfraRed Fluorescence

D1: Dectin-1 receptor

CR3: Complement Receptor 3

REFERENCES

[1] Ahrens ET, Bulte JW. Tracking immune cells in vivo using magnetic resonance imaging. Nat Rev Immunol 2013, 13:755-763.

[2] Long CM, Bulte JW. In vivo tracking of cellular therapeutics using magnetic resonance imaging. Expert Opin Biol Ther 2009, 9:293-306.

[3] Nejadnik H, Castillo R, Daldrup-Link HE. Magnetic resonance imaging and tracking of stem cells. Methods Mol Biol 2013, 1052:167-176.

[4] Wang YX, Xuan S, Port M, Idee JM. Recent advances in superparamagnetic iron oxide nanoparticles for cellular imaging and targeted therapy research. Curr Pharm Des 2013, 19:6575-6593.

[5] Mahmoudi M, Hosseinkhani H, Hosseinkhani M, *et al*. Magnetic resonance imaging tracking of stem cells in vivo using iron oxide nanoparticles as a tool for the advancement of clinical regenerative medicine. Chem Rev 2011, 111:253-280.

[6] Heyn C, Bowen CV, Rutt BK, Foster PJ. Detection threshold of single SPIO-labeled cells with FIESTA. Magn Reson Med 2005, 53(2):312-320.

[7] Bonetto F, Srinivas M, Heerschap A, *et al.* A novel (19)F agent for detection and quantification of human dendritic cells using magnetic resonance imaging. Int J Cancer 2011, 129(2):365-373.

[8] Ferrauto G, Di Gregorio E, Dastrù W, Lanzardo S, Aime S. Gd-loaded-RBCs for the assessment of tumor vascular volume by contrast-enhanced-MRI. Biomaterials 2015, 58:82-92

[9] Geng K, Yang ZX, Huang D, *et al.* Tracking of mesenchymal stem cells labeled with gadolinium diethylenetriamine pentaacetic acid by 7T magnetic resonance imaging in a model of cerebral ischemia. Mol Med Rep 2015, 11:954-960.

[10] Ferrauto G, Di Gregorio E, Baroni S, Aime S. Frequency-encoded MRI-CEST agents based on paramagnetic liposomes/RBC aggregates. Nano Lett 2014, 14:6857-6862.

[11] Ferrauto G, Delli Castelli D, Terreno E, Aime S. In vivo MRI visualization of different cell populations labeled with PARACEST agents. Magn Reson Med. 2013, 69:1703-1711.

[12] Ahrens ET, Zhong J. In vivo MRI cell tracking using perfluorocarbon probes and fluorine-19 detection. NMR Biomed 2013, 26:860-871.

[13] Srinivas M, Boehm-Sturm P, Aswendt M, *et al.* In vivo 19F MRI for cell tracking. J Vis Exp 2013, e50802.

[14] Srinivas M, Morel PA, Ernst LA, Laidlaw DH, Ahrens ET. Fluorine-19 MRI for visualization and quantification of cell migration in a diabetes model. Magn Reson Med 2007, 58:725-734.

[15] Chen J, Lanza GM, Wickline SA. Quantitative magnetic resonance fluorine imaging: today and tomorrow, Wiley Interdiscip Rev Nanomed Nanobiotechnol. 2010, 2:431-440.

[16] Jacoby C, Temme S, Mayenfels F, *et al.* Probing different perfluorocarbons for in vivo inflammation imaging by 19F MRI: image reconstruction, biological half-lives and sensitivity. NMR Biomed 2014, 27:261–271.

[17] Temme S, Bönner F, Schrader J, Flögel U. 19F magnetic resonance imaging of endogenous macrophages in inflammation. Wiley Interdiscip Rev Nanomed Nanobiotechnol, 2012, 4(3):329-343

[18] Temme S, Jacoby C, Ding Z, *et al.* Technical advance: monitoring the trafficking of neutrophil granulocytes and monocytes during the course of tissue inflammation by noninvasive 19F MRI. J Leukoc Biol 2014 95(4):689-697.

[19] Ahrens ET, Helfer BM, O'Hanlon CF, Schirda C. Clinical cell therapy imaging using a perfluorocarbon tracer and fluorine-19 MRI. Magn Reson Med 2014, 72(6):1696-1701.

[20] Huang H, Ostroff GR, Lee CK, Specht CA, Levitz SM. Characterization and optimization of the glucan particle-based vaccine platform, Clin Vaccine Immunol. 2013, 20:1585-1591.

[21] Soto ER, Caras AC, Kut LC, Castle MK, Ostroff GR. Glucan particles for macrophage targeted delivery of nanoparticles, J Drug Deliv 2012, 2012:143524.

[22] Tesz GJ, Aouadi M, Prot M, *et al.* Glucan particles for selective delivery of siRNA to phagocytic cells in mice. Biochem J 2011, 436(2):351-362.

[23] Aouadi M, Tesz GJ, Nicoloro SM, *et al.* Orally delivered siRNA targeting macrophage Map4k4 suppresses systemic inflammation. Nature 2009, 458:1180-1184.

[24] Figueiredo S, Cutrin JC, Rizzitelli S, *et al.* MRI tracking of macrophages labeled with glucan particles entrapping a water insoluble paramagnetic Gd-based agent. Mol Imaging Biol 2013, 15:307-315.

[25] Garello F, Stefania R, Aime S, Terreno E, Delli Castelli D. Successful entrapping of liposomes in glucan particles: an innovative micron-sized carrier to deliver water-soluble molecules. Mol Pharm. 2014, 11:3760-3765.

[26] Garello F, Arena F, Cutrin JC, et al. Glucan particles loaded with a NIRF agent for imaging monocytes/macrophages recruitment in a mouse model of rheumatoid arthritis. RSC Adv 2015, 5:34078-34087.

[27] Waiczies H, Lepore S, Janitzek N, *et al.* Perfluorocarbon Particle Size Influences Magnetic Resonance Signal and Immunological Properties of Dendritic Cells. Plos ONE 2011, e21981.

[28] Soto ER, Ostroff GR. Characterization of Multilayered Nanoparticles Encapsulated in Yeast Cell Wall Particles for DNA Deliver. Bioconj Chem 2008, 19:840–848.

[29] Figueiredo S, Moreira JN, Geraldes CF, Rizzitelli S, Aime S, Terreno E. Yeast cell wall particles: a promising class of nature-inspired microcarriers for multimodal imaging. Chem Commun 2011, 47(38):10635-10637.

[30] Janjic JM, Srinivas M, Kadayakkara DKK, Ahrens ET. Self-delivering Nanoemulsions for Dual Fluorine-19 MRI and Fluorescence Detection. J Am Chem Soc 2008, 130:2832-2841.

[31] Brown GD, Gordon S. Immune recognition: a new receptor for β-glucans. Nature 2001, 413:36–37.

[32] Huang H, Ostroff GR, Lee CK, Agarwal S, Ram S, Rice PA *et al*. Relative contributions of Dectin-1 and complement to immune responses to particulate β-glucans. J Immunol 2012, 189:312–317.